Article

JOURNAL OF COMPOSITE MATERIALS

Journal of Composite Materials
2026, Vol. 60(13) 1239–1251

DOI: 10.1177/00219983251384008
journals.sagepub.com/home/jcm
Sage

Preparation and characterization of composite interference screws

Safa Kararmaz[1], Fatma Duygu Garip Celik[2], Alkin Ozgen[1], Orhan Gokalp Buyukuysal[1], Cagdas Hakki Basat[3], Faruk Mert[4] and Halil Murat Aydin[1,5]

Abstract

The Anterior Cruciate Ligament (ACL) is an important connector between the thigh bone and shinbone in the knee joint. In sport activities, ACL tears commonly occur hence they need surgery to be rebuilt. These are patellar tendons located in front of the knee and hamstring tendons found on its posterior side that are mostly used for reconstruction of the anterior cruciate ligament. These grafts can be secured by using bioabsorbable interference screws by surgery. Here we report development of composite interference screws consisting of 70% (w/w) Poly (Lactic Acid-*co*-Glycolic Acid) (PLGA) and 30% (w/w) β-Tricalcium Phosphate (β-TCP) with different sizes using plastic injection molding. A series of characterization techniques was used to validate the final product including Thermal Gravimetric Analysis, Fourier Transform Infrared Spectroscopy, Inductively Coupled Plasma Mass Spectrometry, Scanning Electron Microscopy. Interference screws were tested mechanically and finally biocompatibility was investigated. The studies carried out here are thought to contribute to a better understanding of the screws used in the treatment of cruciate ligament injury and new biomaterials that can be developed for treatment.

Keywords

anterior cruciate ligament, polymer composite, interference screw, poly (lactic acid-co-glycolic acid) (PLGA), β-tricalcium phosphate (β-TCP)

Highlights

Polymer-ceramic biodegradable composite interference screws have become prominent in anterior cruciate ligament surgeries.

In this study, 70/30% (w/w) PLGA and β-TCP composites were used to produce interference screws of different lengths and diameters.

The interference screws were evaluated physically, chemically, morphologically and biologically.

Addition of ceramic phase is believed to enhance the mechanical properties of the final composites and eliminates the detrimental effects of polymer degradation by balancing the pH.

Introduction

It is very important to have information about knee anatomy in order to understand and overcome problems in cruciate ligament injuries. The knee is a complex joint formed with the participation of three bones and many ligaments. Another feature that makes the knee special is that the knee is the largest joint in the body and consists of the combination of two joints (tibiofemoral and patellofemoral).[1]

When the knee joint is examined, it is seen that there are ligaments responsible for the stabilization of the joint and the coordination of movements. These ligaments can basically be classified as anterior, posterior and lateral cruciate ligaments. The ACL has an average size of 30-32 mm in

[1]Bioengineering Division, Institute of Science, Hacettepe University, Ankara, Turkey
[2]BMT BAPS Biomaterial Co., Ankara, Turkey
[3]Orthopedics and Traumatology Division, Medical School, Kirsehir Ahi Evran University, Kirsehir, Turkey
[4]Vocational School of Technical Science, Ankara Yildirim Beyazit University, Ankara, Turkey
[5]Centre for Bioengineering, Hacettepe University, Ankara, Turkey

Corresponding author:
Halil Murat Aydin, Institute of Science, Bioengineering Division and Centre for Bioengineering, Hacettepe University, Ankara 06800, Turkey.
Email: hmaydin@hacettepe.edu.tr

Data Availability Statement included at the end of the article

length and 7–11 mm in diameter. Its main task is to help stabilize the tibia.[2]

The main function of the ACL is to stabilize the knee anteriorly. Since this ligament does not have regeneration, it is necessary to reconstruct it by various methods. The most popular method today is arthroscopic repair using autogenous Hamstring tendon graft. An issue as important as the graft and method used is the graft fixation technique. The use of tunnel-free fixation or in-tunnel fixation (with interference screws) methods are important for the stability of the fixation. Widely used materials for the interference screws are metals (titanium, magnesium, stainless steel), polymers, ceramics and composites.[3] Polymers are among the materials used in implant production in the field of orthopedics. Absorbable polymers such as Polyethene and Polymethylmethacrylate are also quite common and have irreplaceable uses. Second generation bioactive and biodegradable polymers allow controlled degradation of their chains. Poly (lactic acid) (PLA), Poly (glycolic acid) (PGA), PLGA, Poly (L-lactic acid) (PLLA), Poly (p-dioxanone) (PDS), Poly (ε-caprolactone) (PCL), Poly (hydroxybutyrate) (PHB), Poly (2-hydroxyethyl-methacrylate) (PHEMA), Chitosan, Hyaluronic Acid are biodegradable and bioactive.[4] These second-generation polymers have been used in many orthopedic applications to repair bone fractures as bone substitutes.[5] Polymers such as PGA, PLA and their copolymers are also bioabsorbable. Cells begin to proliferate by adhering to the bioabsorbable polymer and produce their own extracellular matrix (ECM). Until target tissue healing is completed, bioabsorbable polymers provide a suitable environment for cells. However, the known risks of foreign body reaction caused by PGA and its effect on synovitis and effusion resulted in a decrease in its usage.[6] Also, PGA screws can fail to restore the stability and tissue healing due to their rapid resorption rate.[7]

Another type of biomaterial commonly used in orthopedics is ceramics. The formulation range of these materials is limited. Parameters such as particle size and distribution, porosity, production temperature, powder purity are important in the production process of ceramic materials. Second generation ceramics are biodegradable. Among these ceramics, bioglasses (BG) and Calcium Phosphates (CaP) are at the forefront. These materials exhibit surface properties similar to bone tissue. The bonding strength between the ceramic material and bone is high.[8,9] Calcium phosphate groups can exist in different forms depending on impurities and the presence of water, as well as depending on the production temperature. Bioactivity grade and degradation behaviors generally depend on the calcium/phosphorus (Ca/P) ratio, purity of phases and crystallinity. These ceramics show hardening behavior in the lowest amount of heat formation inside the damaged bone tissue to which it is applied. One of the most commonly used bioceramics are Hydroxyapatite, β-TCP and their derivatives.[10–13] Upon the creation of a composite structure, by combining a bioceramic phase with biodegradable polymer several advantages can be achieved. The initial one is that this improves mechanical properties of the final construct. This increases the controllability of polymer degradation process.[14] Ceramic particles such as Hydroxyapatite or β-TCP combined with a biodegradable polymer like PLGA from physicochemical viewpoint provides pH buffering effect to optimize degradation and absorption kinetics of composite structure. Consequently, degradation rate of composite structure is controlled thus avoiding the formation of acid environment harmful to cells. In conclusion, this control helps reduce inflammatory response towards acidic byproducts such as inflammation which may be released from the decomposing polymers.[15,16]

The first designs of interference screws were metal and were used successfully at that time because they had sufficient mechanical strength as implantation materials.[17] In the following period, interference screws were produced using PLA and copolymers. These screws have the advantages of drillability at the time of implantation and magnetic resonance imaging (MRI) compatibility. Screws obtained from biodegradable polymers are equivalent to metal screws in terms of mechanical strength.[18,19] In studies focused on PLA and especially PLLA, it was aimed to optimize the time due to the time-consuming degradation process. In order to eliminate this situation, stereoisomers of PLA and copolymers combined with PGA have been developed.[20–23] Although these stereoisomers and copolymers achieve faster degradation times, no bone formation has occurred in the use of this materials. Biocomposites consisting of a biodegradable polymer (PLGA) and a ceramic material (β-TCP) were studied to achieve a better recovery process. This composite structure maximizes osteoconductivity while minimizing the risk of inflammation. In addition, there is an increase in mechanical strength. The interference screw's composite structure, consisting of 70/30% PLGA/β-TCP by weight, ensures the desired level of time-dependent degradation and tissue healing. The PLGA/β-TCP used in this model provides a longer degradation time, allowing sufficient time for tissue healing to occur fully. This advantage allows the screw to resist the necessary biomechanical pressures while also being biodegradable. This allows the screw to not only facilitate cell migration but also provide suitable surfaces for cell attachment, facilitating proliferation, tissue formation, and repair. This composite biomaterial has been reported to have the highest rates of osteoconductivity reported in the literature.[24–26] Moreover, to prevent biodegradable composite devices from breaking during the insertion of implants, and also to prevent the acidity of the degradation products from resulting in inflammatory and foreign body reactions, a new approach with different weight ratios is crucial.[27]

In addition to the components and biomechanical compatibility contained in the material, it is important to

consider geometry in interference screws. The geometric properties of the screw (outer and inner diameter, length, gap size, support geometry) are critical in its interaction with the tissue. In general, the greater the area of contact with the screw teeth on the bone surface, the more successful the fixation has been reported. For this reason, design studies are of great importance.[28–33] In this study, a novel biodegradable interference screw was designed using PLGA and β-TCP composite.

Experimental

Determination of the raw material

Within the scope of the study, 70/30 (w/w) PLGA/β-TCP composite raw materials (purchased from BMT BAPS Biomaterial Co.) were used. The raw material was decided by conducting comparative literature research on the basis of interference screws. The percentage of the components of PLGA polymer and β-TCP ceramic phase was also shaped according to literature studies.

Design studies and prototype production

Composite interference screws with lengths of 25 mm and 30 mm and a diameter range of 6–11 mm have been designed and finalized in a dimensional and vector-based three-dimensional form using the SolidWorks program. Among the composite intervention screws, the prototype with a length of 30 mm and a diameter of 11 mm was deemed appropriate to use. To improve the product design, a preliminary evaluation process was carried out using a 3D Printer and revisions were made, taking into account equivalent products. During the renovation work, the design was revised by taking the ASTM F543 (Standard Specification and Test Methods for Metallic Medical Bone Screws) standard as a reference and its final shape was given taking into account ease of application. Plastic injection moulding process was done with Babyplast 6/10 (Germany) device. After the final design of the composite interference screw, a mold was made and then prototype production started.

Test protocols

The composite interference screws were characterized thermally, chemically, physically, morphologically and biologically. Thermogravimetric Analysis (TGA), Differential Scanning Calorimetry (DSC) and Fourier Transform Infrared (FTIR) Spectroscopy procedures are given in the Supplemental Information (SI).

Chemical analysis. Inductively Coupled Plasma Mass Spectrometry (ICP-MS) analysis was performed to analyse the presence of elemental residues in the sample and to determine the impurity, if any. This analysis was performed for heavy metals (As, Hg, Cd, Pb) with Perkin Elmer DRC II Model ICP-MS device (USA) in accordance with ASTM F 1088 standard. The X-Ray Diffraction (XRD) analysis was performed in the Rigaku Ultima-IV X-Ray Diffraction device (Japan). XRD analysis was carried out to observe the effects of sterilization process and accelerated ageing on the ceramic phase in the composite material. The measurement was carried out at a scan rate of 1°C/minute, at the sampling step of 0.02°, in 2θ measuring axes, 20–90° scanning range, using copper (Cu) welding at Kα = λ = 1.54 Ang., 40 kV, 30 mA.

Morphological analysis. Scanning Electron Microscopy (SEM) analysis was performed to obtain surface images of the produced composite interference screw and to prove that the polymer ceramic phases show a homogeneous distribution on the screw surface. Since the screw dimensions are larger than the measuring chamber, SEM analysis was performed on a piece without deformation after the screw was divided into small pieces. Images were acquired in QUANTA 400F Field Emission Scanning Electron Microscope (Austria) at 30×, 100×, 250×, 1000× and 2000× magnifications at 1.2 nm resolution. Computed Micro Tomography (Micro-CT) analysis was performed on Bruker SkyScan 1275 (USA) device at 125 milliamps at 80 kV in a 10 μm cross section range, and 1 mm thick aluminium filter was used during imaging. In order to obtain optimum quality image from the device, rotation step 0.2, radiation exposure time 49 ms per shot and frame average setting fixed to 6. Images were obtained in 2D and 3D, and presented in colour with related software.

In Vitro *Degradation and mechanical test analysis.* *In vitro* degradation test was performed on the composite interference screws Ø11–L30 according to the guidelines of ISO 13781:2017 Standard. The degradation experiment was carried out in a 37°C incubator in sorensen buffer solution. The results of the 6-months degradation experiment were evaluated under the related topic in the Results and Discussion section. TGA analysis data for the characterization of T_0, T_3 and T_6 months, DSC analysis data, inherent viscosity values, mass losses and morphological changes were investigated. During the degradation test period, static torsion analysis was also performed to observe whether there was any change in mechanical strength. Mechanical tests were performed with the Bruker's Universal Mechanical Tester device (USA). In the mechanical test analysis of the samples, the values such as average torsional yield strength (N.m), average maximum torque (N.m), and mean break angles of the moments of T_0, T_3 and T_6 were evaluated. The breaking points of the screws during the experiment set were included in the study visually. The test speed was determined as 3 cycles/minute and the axial preload was −50 N under the test conditions. Storage conditions was selected as 50 ± 5% (humidity) and 23 ± 2°C

(temperature) for accelerated aging studies. The screws were adapted to the system with 20% thread length exposed and torsional force was applied to the screws until fail. In addition to these tests, static torsion analysis was performed on composite interference screw with dimensions Ø7–L30. This test was built and evaluated to predict and display the mechanical values of composite interference screws with other diameter sizes planned to be obtained using the iteration method. Testing was carried out in laboratory conditions at 25°C and 50% humidity. The mechanical test analysis results obtained during the degradation at T_0 are included in the Results and Discussion section.

Biocompatibility analysis. The composite interference screw was subjected to biocompatibility tests planned according to ISO 10993 Biological Evaluation of Medical Devices. All biocompatibility testing was conducted at ISO 9001: 2015 certified APT Testing and Research Private Limited. The results of the tests are presented under the relevant heading in the Results and Discussion section.

In vitro cytotoxicity study was carried out following the guideline ISO:10993-1:2018(E)-Part-1, ISO:10993-5: 2009(E)-Part-5, ISO:10993-12:2012(E)-Part-12. The study was conducted to determine the *in vitro* cytotoxic potential of interference screws test material against L-929 mammalian fibroblast cells by direct contact method. All cultures were examined under an inverted microscope to elucidate changes in cell morphology.

Intracutaneous (intradermal) polar and non-polar reactivity test was performed following the guideline ISO: 10993-1:201S(E)-Part-1, ISO:10993-02:2006(E)-Part-2, ISO:10993-10:2010(E)-Part-10, ISO:10993-12:2012(E)-Part-12. The study was conducted to determine the skin irritation potential of normal saline (polar) extract and sesame oil (non-polar) extract of interference screw test material on rabbits. Polar extract was administered intravenously and non-polar extract was administered intraperitoneally. Three New Zealand White Rabbits were used for this study. Injection sites were observed at 24, 48 and 72 h for signs of erythema, oedema and necrosis.

Pyrogen test was performed following the guideline ISO: 10993-1:2018(E)-Part-1, ISO:10993-02:2006-Part-2, ISO: 10993-11:2006(E), ISO:10993-12:2012(E)-Part-12. The Pyrogen Test study was carried out to determine the pyrogenicity of interference screw in rabbits after intravenous administration of the test material.

Bone implantation was performed following the guideline ISO:10993-1:2018(E)-Part-1,ISO:10993-02:2006(E)-Part-2, ISO:10993-6:2016(E)-Part-6, ISO:10993-12(E)-Part-12. Bone implantation study aimed to determine the local effects of the interference screw test material after 14 days of implantation into rabbit bone. The test material was implanted into SS316 L bone in rabbits. The rabbits were observed for 14 days. The bone contact area was evaluated macroscopically and microscopically for the amount of bone around the implant, the presence of non-calcified tissues and inflammatory changes.

Guinea Pig Maximization Test (GPMT) study was conducted to determine the skin sensitization potential of interference screw test material in guinea pigs following the GPMT according to ISO:10993-1:2018(E)-Part-1, ISO: 10993-02:2006(E)-Part-2, ISO:10993-10:2010(E)-Part-10, ISO:10993-12:(E)-Part-12. Ten animals were treated intradermally with the test extracts and five animals were used as controls. Skin reactions at the site of application were recorded periodically.

Sub-chronic systemic toxicity test was performed following the guideline ISO:10993-1:2019(E)-Part-1, ISO: 10993-02:2006(E)-Part-2, ISO:10993-6:2016(E)'-Part-6, ISO:10993-11:2017(E)-Part-11, ISO:10993-12: 2012 (E) Part-12. Sub-chronic systemic toxicity test aimed to determine the sub-chronic systemic toxicity of the interference screw according to the implantation route (13 weeks). The test material was implanted into the femur of four male and four female rabbits. Similarly, the USP HDP RS negative control was implanted in four male and four female rabbits. The animals were observed for 13 weeks. At the end of the 13 weeks, blood was collected for the determination of blood chemistry and hematologic parameters. The implant tissues were examined macroscopically and microscopically. All animals were observed for signs of irritation and toxicity.

Genotoxicity study aimed to determine the genotoxicity of the interference screw test material in CHO mammalian fibroblast cells following ISO-10993-3:2014/ OECD473 Guidelines. Cells were collected from CHO mammalian fibroblast cells and incubated in Ham's F12 medium supplemented with 10% fetal calf serum for 2 h at 37°C. All cultures were examined under a microscope for changes in cell morphology.

The hemocompatibility study was conducted to determine the hemocompatibility of interference screw test material following ISO 10993-4:2017(E) Guidelines. Three samples of the test material were incubated for 1, 2 and 4 h at 37°C in sterile containers in contact with human blood of blood group A+, B+ and 0+ respectively.

Bacterial mutation testing was performed to assess the potential of the test product to induce point mutations in various test strains of *Salmonella Typhimurium* that restore the functional capacity of the bacteria. In keeping with the ISO-10993-3:2014 regulations, a polar extract of the test substance was made at 0.20 g/mL by autoclaving it for 1 h at 121°C. This extract was then subjected to an Ames/ Salmonella plate incorporation assay in order to check on its capability to cause reverse mutation of selected cell lines.

Results and discussion

Thermogravimetric Analysis (TGA), Differential Scanning Calorimetry (DSC) and Fourier Transform Infrared (FTIR)

Spectroscopy were used to confirm the prepared structure. The thermal stability of PLGA/β-TCP composite was determined by TGA. According to the results of the analysis, 70.45 ± 1 wt% PLGA degraded in composite interference screw. The results are consistent with the TGA analysis results of PLGA composites with different TCP content in the literature.[34] The results of the characteristic properties of the composite such as T_{start} (°C, initial degradation), T_{max} (°C, maximum degradation) were found to be consistent. The main reason for the differences is the β-TCP content. In addition, variables such as the shape of the composite and injection parameters may also have caused differences. According to the TGA analysis results, it is seen that the 2-years accelerated aging test does not affect the thermal character of the screw.

The main thermal parameter values of screw and the stability of the thermal character are shown by DSC analysis. No clear crystallization peak was observed in the double-heated test result graph. The glass transition temperature (T_g) represents the baseline displacement of the material in the DSC graph. The melting temperature point (T_m) of the raw material was found 157.97°C. The melting temperature point (T_m) at which the sterile screw started to melt in the first heating was determined as 161.39 ± 1°C. The melting temperature (T_m) point of 162.16 ± 1°C for the first heating and the temperature point of 155.33°C for the second heating is the point where the 2 years accelerated aged screw material begins to melt. The melting temperature point (T_m) is the second peak observed in the DSC curve. The high T_m value of 157.97°C for the raw material may indicate the presence of a crystalline structure. This can be explained by the presence of crystals in very close and regular structures. Literature shows that polymers containing less than 10% L-lactide monomer tend to form amorphous structures.[35–38] In this context, it can be inferred that the L-lactide monomer content in the raw material is more than 10%. In previous studies, the glass transition temperature (T_g) for pure PLGA was reported as 59.49°C and the melting temperature (T_m) as 155.39°C. The glass transition temperature (T_g) of the raw material in our study was found 66.79°C. It is expected that the glass transition temperature (T_g) increases with the addition of β-TCP. This is likely to occur as a result of the interaction of β-TCP particles with PLGA matrix. Due to this interaction, the mobility of PLGA chains decreases.[39] The glass transition temperature (T_g) of the sterile screw was 61.12°C for the first heating, 51.35°C for the first cooling, 52.36°C for the second heating, respectively. The glass transition temperature (T_g) of the 2-years accelerated aging screw was 60.40°C for the first heating, 50.85°C for the first cooling, 56.12°C for the second heating, respectively. It was determined that there was no significant difference in the results obtained. Therefore, it was concluded that the aging process accelerated by 2 years did not affect the thermal character of the material.

In the result of FTIR analysis, the (-P-O-) single bond and (-P = O-) double bond appears in the bands at 945 cm^{-1}, 970 cm^{-1} and these two peaks are evidence for the presence of pure β-TCP. The characteristic carbonyl peak (-C = O-) of PLGA polymer is observed in the 1748 cm^{-1} band. There are CH, CH_2 and CH_3 stretching vibrations between the characteristic PLGA bands at 2947 cm^{-1}, 2997 cm^{-1}.[40] These data can be shown as evidence for the presence of PLGA.

Chemical analysis – ICP - MS (inductively coupled plasma mass spectrometry)

The results of the ICP-MS test in the raw material used, the element lead (Pb) has been determined as 0.58 ± 0.03 ppm and the element cadmium as 0.19 ± 0.01 ppm. The elements arsenic (As) and mercury (Hg) were found to be below the limit of detection. ASTM F 1088 standard, the maximum concentration limit for lead element is 30 ppm, the maximum concentration limit for cadmium (Cd) element is 5 ppm, the maximum concentration limit for arsenic element is 3 ppm and the maximum concentration limit for mercury element is 5 ppm. It is stated that the total heavy metal concentration can be maximum 50 ppm (Table 1). These results, the concentration of heavy metals in the raw material to be used in composite interference screws was in the appropriate range per ASTM F 1088 standard.

Chemical analysis - XRD (X - ray diffractometer)

The qualitative analysis results, the analysed sample contains $Ca_3(PO_4)_2$ (Tri-Calcium Phosphate) groups. $Ca_3(PO_4)_2$ peaks shown in the diffraction file of the $Ca_3(PO_4)_2$ located in the International Center for Diffraction Data have been matched with the peaks in the XRD analysis of the screw we obtained. The bottom graph in Figure 1 is the XRD reference

Table 1. ICP-MS analysis of raw material.

Raw material	Element amount (mg/kg) (ppm)	Maximum limit according to ASTM F 1088 standard (ppm)
Pb	0.58 ± 0.003	30
Cd	0.19 ± 0.01	5
As	Not detected	3
Hg	Not detected	5

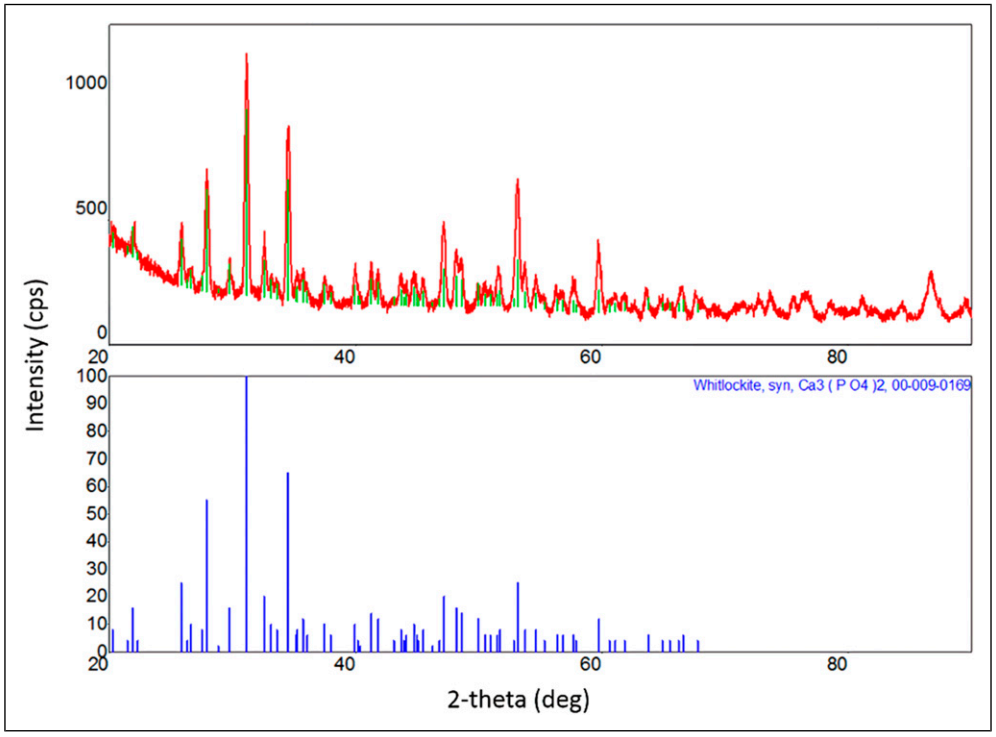

Figure 1. Diffractogram of sterile screw (top) and $Ca_3(PO_4)_2$ powder diffraction card (bottom).

card in the file with the card number 00-009-0169 PDF (Powder Diffraction File). It is shown in Figure 1 that the peaks match exactly to that of reported in literature.[41] In addition, it shows agreement with the XRD spectrum of PLGA-TCP composite at the same ratios.[42]

The peaks in the 5th, 7th, and 11th are the largest length in the chart. The crystal size of the largest peak (peak in the 7th row), calculated using Scherrer's formula, can be considered as the average size of the crystals in the composite interference screw.[43] These results, the size of the crystals in the screw content was accepted as an average of 28 nm along with the margin of error.

Morphological analysis - SEM (scanning electron microscope)

SEM images (Figure 2) are in different magnifications taken for the surface of the composite interference screw sterilized with ethylene oxide. In these images, it is examined whether the ceramic and polymer phases forming the screw have a homogeneous distribution on the screw surface.

In Figure 2, the general view of the grooves on the outer surface of the screw in image (a) at 30× magnification was taken. Image (b) focuses on a single groove; the image was taken at 100× magnification to make the groove more prominent. In image (c), the image of the recess region between the groove and the screw surface at 250× magnification was recorded. The brighter region indicates the groove recess region, and the darker area to the right belongs to the upper part of the groove. The image in the lower right (d) shows the surface area between the grooves on the outer surface of the screw at 250× magnification. Images were taken in image (e) and (f) at 1000× and 2000× magnifications, respectively. These images belong to the outer surface of the screw. These magnifications have been examined in order to distinguish the components in the screw in more detail and to determine whether there is a homogeneous distribution. The particles that appear brighter in the images belong to the β-TCP ceramic phase. The darker regions are the regions showing the PLGA polymer. In the (g) and (h) images obtained at 1000× and 2000× magnifications, respectively, whether the components are homogeneously distributed on the inner surface of the screw is examined. As a result of the examination of the images, it was evaluated that the components show a homogeneous distribution on the surfaces. SEM images obtained during the degradation study are evaluated separately in the results and discussion section under the title *In Vitro* Degradation and Mechanical Test Results.

Morphological analysis - μ-CT (micro-computed tomography)

Figure 3 shows 3D images of the screw and 2D radiopacity scanning. According to these images, channel and groove structures suitable for the design have been seen. In the 2D

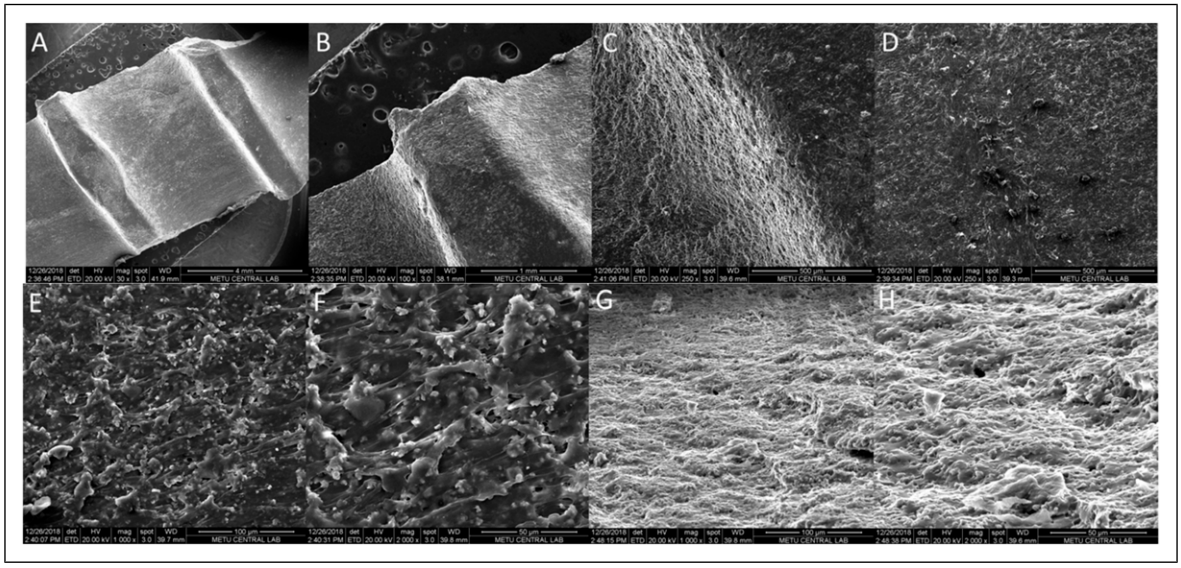

Figure 2. SEM images of sterile screw. (a) 30×, (b) 100×, (c) 250×, (d) 1000×, (e) 2000×, (f) 2000×, (G) 1000× magnification. a, b, c and d images are inner surface of the screw while e, f, g and h images are outer surface of the screw.

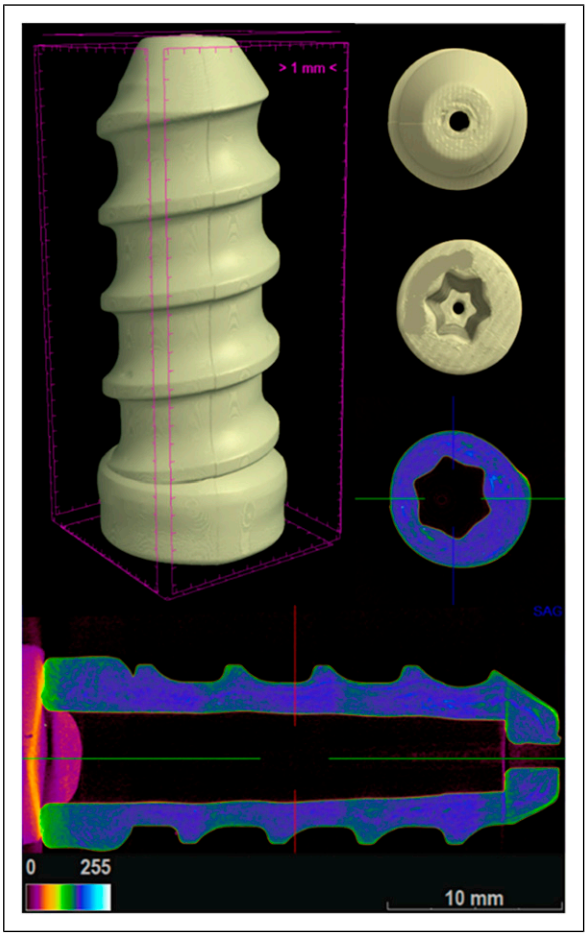

Figure 3. 3D Images and 2D radiopacity scan image of composite interference screw after sterilization process.

image (bottom right), the components in the composite structure have been shown to show a homogeneous distribution. When these images and the surface images obtained by SEM analysis are correlated, it can be said that the surface has a regular structure, PLGA polymer phase and β-TCP ceramic phase exhibit a homogeneous distribution. In these images of the screw, it is seen that the screw is not adversely affected by heat treatment during production in the plastic injection moulding device, has dimensions, grooves and groove structure suitable for the design, and this structure has a homogeneous distribution of components. In order to calculate the mineral density of the sample, hydroxyapatite rods with the same thickness and 0.25 and 0.75 g/cm^3 densities were scanned and reconstructed at the same settings as the sample. After the analysis program related to the images obtained from these bars was calibrated, the mineral density of the sample was determined as 121.7 g/cm^3. In the detailed analysis of the sample in.bmp format with special software, the volume of the object was determined as 1696.9 mm^3. In the sample with 99.99% substance density, 557 closed pores were detected, and these pores constitute 0.00117% of the sample. The total volume of these closed pores was determined to be 0.0109 mm^3. It has been shown that two different radiopacity components shape the sample, and the sample that holds more space by volume in these components has a volume of 95.96% by volume compared to the total.

In vitro *degradation and mechanical test*

In vitro *degradation.* *In vitro* degradation test has been made according to ISO 13781:2017 to the composite interference screw with Ø11–L30 dimensions. During this test, weight

change (%), size (dimension) change (%), glass transition temperature (°C), water content (%), inherent viscosity (dL/g) and roughness were evaluated. The results of this 6-months study at T_0, T_3 and T_6 times are given in Table 2.

According to the the results, the total weight also increases since the amount of water in the material increases, and accordingly the inherent viscosity decreases. As seen in Table 2, a total weight increase of 3.75% occurred in the material within 180 days. In addition to this, an increase of 1.36% amount of water occurred.

During the degradation process, weight loss increases with the increase in water content as a result of the erosion of β-TCP and the breaking and disintegration of the molecular chains of PLGA by water molecules which seep into the polymer structure and attack the ester bonds.[48] Thus, a decrease in inherent viscosity is expected.

In the literature, it has been reported that the inherent viscosity of a PLGA/β-TCP (70:30) screw decreased from 100% to around 25% after 6 months of degradation.[44] The inherent viscosity rate of the screw with the same composition percentage in our study decreased from 100% to 35.25%. The reason behind the slower decreased inherent viscosity compared to the literature study is that the screw in our study has less water content and therefore less weight loss as a result of relatively slower degradation. In this step, there is a loss of molecular weight but no change in physical appearance (in the macro level).

The screw must remain in the body for a long time and be able to withstand the necessary mechanical loads while degrading. Since inherent viscosity is a measure that determines the internal resistance and molecular weight of the implant, its excessive decrease may indicate an irregularity or fragmentation in the molecular structure. This structural degradation can negatively affect the durability and mechanical properties of the material. Sufficient decomposition time of our composite structure allows tissue healing to be at the desired level. A longer decomposition time will provide enough time for tissue healing to take place completely.

During the degradation of pure PLGA on day 42, water uptake increased to approximately 2%. When the tricalcium phosphate ratio of doped PLGA was increased to 10%, 20% and 30%, the water uptake increased to 3%, 4%, 9% and 13%, respectively. However, since their standard deviations are high, these rates drop to 2%, 3%, 6% and 8%.[46]

When the degradation performance of the screw is evaluated in the light of these values, the inherent viscosity, water absorption, weight change results are within the desired range, as the screw must provide long-term stability while degrading.

As a result of the 180-days degradation experiment, no changes were observed in the dimensional measurement and surface roughness values. The glass transition temperatures obtained in this 6-months study are consistent. In the degradation study, our material in liquid medium begins degradation by hydrolysis of ester bonds. The contact of the ambient fluid with the amorphous region during hydrolysis causes ruptures in the van der Waals and hydrogen bonds. This causes the glass transition temperature to drop.[45] When the reference study[47] is examined, it is seen that the initial T_g temperature of the material used is lower than the initial value of the prepared Ø11–L30 composite interference screw. This was found to be acceptable since the material we produced in our study is a composite structure. The T_g values presented in the DSC analysis of the composite interference screw are consistent with the T_g values obtained during the degradation process.

SEM images obtained for T_0 (initial), T_3 (3-months degradation) and T_6 (6-months degradation) are given in Figure 4(a) and (b) images belong to moment T_0, (c) and (d)

Table 2. Degradation results, acceptance criteria (references) and comparison chart.

Characterization values	T_0 = Initial Ø11-L30 PLGA/β-TCP (70:30 w/w)	T_3 = 3 Month Ø11-L30 PLGA/β-TCP (70:30 w/w)	T_6 = 6 Month Ø11-L30 PLGA/β-TCP (70:30 w/w)	Literature Refence PLGA (various ratios)
Weight change (%)	N/A	1.5	3.75	T = 24th week 1[44]
Glass transition temperature T_g (°C)	60°C	58°C	57°C	T_0 >37°C[45]
Water content (%)	0.24	0.86	1.36	T = 3th week 6–11[46] T = 6th week 8–13[46]
Inherent viscosity (25°C) dL/g	1.56	1.05	0.55	T_0 0.54[47]
Roughness (μm)	25	25	25	-

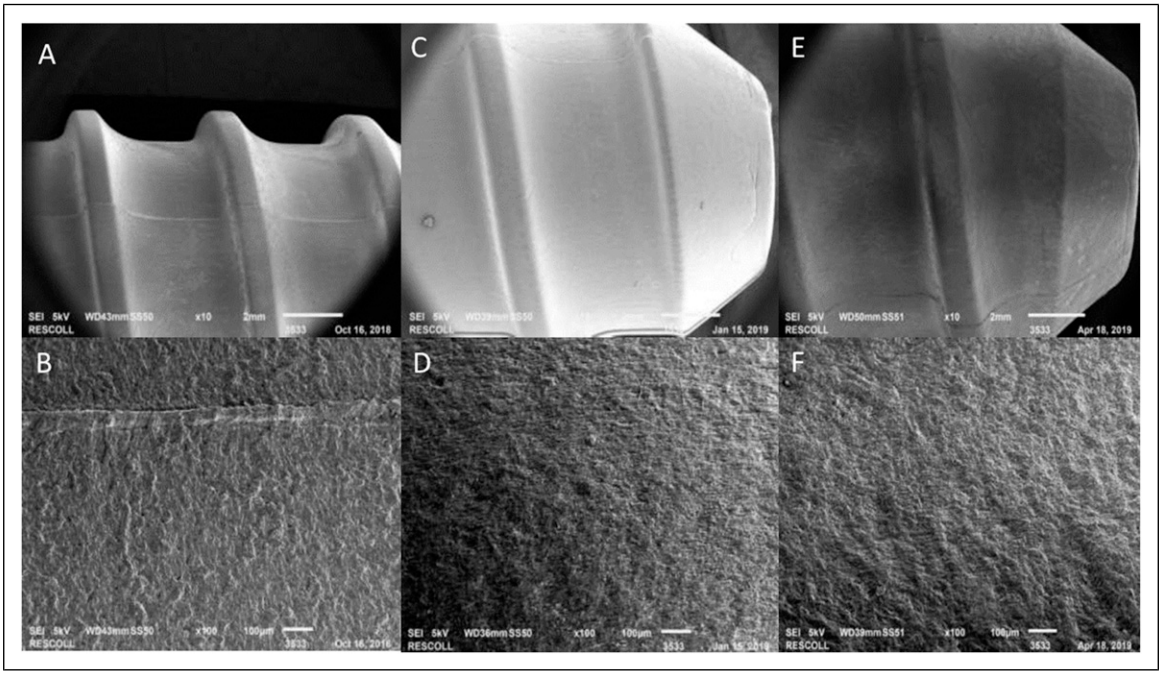

Figure 4. SEM images obtained for T_0 (initial), T_3 (3-months degradation) and T_6 (6-months degradation) moments. (a) and (b) images belong to moment T_0, (c) and (d) images belong to moment T_3, (e) and (f) images belong to moment T_6. The top images were taken at 10× magnification, the bottom images at 100× magnification.

images belong to moment T_3, and (e) and (f) images belong to moment T_6. Images were taken in image (a), (c) and (e) at 10× magnifications; image (b), (d) and (f) at 100× magnifications, respectively. In the images obtained in the periods specified in the 6-months study, there was no visible difference on the surface.

Considering that the water absorption and weight loss data of the screw are relatively low, it has been observed that the degradation of the screw progresses slowly. The fact that the surface roughness is stable at moments T_0, T_3 and T_6 also supports these results. The advantages of relatively slow degradation are discussed in the section above. As a result of interpreting these data with the literature, it was found normal that no significant change was observed in the SEM images.

Mechanical test analysis during in vitro *degradation experiment.* In addition to the tests applied to the composite interference screw with Ø11–L30 dimensions, mechanical tests were performed on the prepared composite interference screw with Ø7–L30 dimensions at T_0. In addition, mechanical values of our materials with diameters of 8 mm, 9 mm, 10 mm were tried to be predicted by iteration method. When the values obtained for the selected test specimen are examined, the maximum torque and torsional yield strength values at T_0, T_3 and T_6 for the composite interference screw with Ø11–L30 dimensions were determined as 6.6 N.m (SD 0.2)–6.2 N.m (SD 0.6), 4.8 N.m (SD 0.9)–4.6 N.m (SD 0.8), and 3.59 N.m (SD 1.16)–3.40 N.m (SD 1.2) respectively (Table 3). The torsional yield strength and maximum torque values of the specimens decreased significantly after 3 and 6 months of degradation. According to the results, it can be interpreted that β-TCP particles started to separate from the PLGA matrix especially after 3 months of degradation. It has been reported in the literature that increasing β-TCP content significantly increases the mechanical strength of PLGA.[49] In this context, decreasing mechanical strength can be associated with decreasing β-TCP content. During the 6-months degradation period, the decrease in mechanical properties became more pronounced.

In the degradation study, three screws did not break in the torsion test performed on eight screws in the T_0 initial

Table 3. Comparison chart of mechanical test results obtained at T_0, T_3, T_6 during the degradation test process (SD: standard deviation).

	Ø11–L30–(T_0)	Ø11–L30–(T_3)	Ø11–L30–(T_6)
Torsion yield strength (N.m)	6.2 ± 0.6	4.6 ± 0.8	3.40 ± 1.2
Maximum torque (N.m)	6.6 ± 0.2	4.8 ± 0.9	3.59 ± 1.16
Angle of recracting (°)	43 ± 8	54 ± 23	20 ± 5

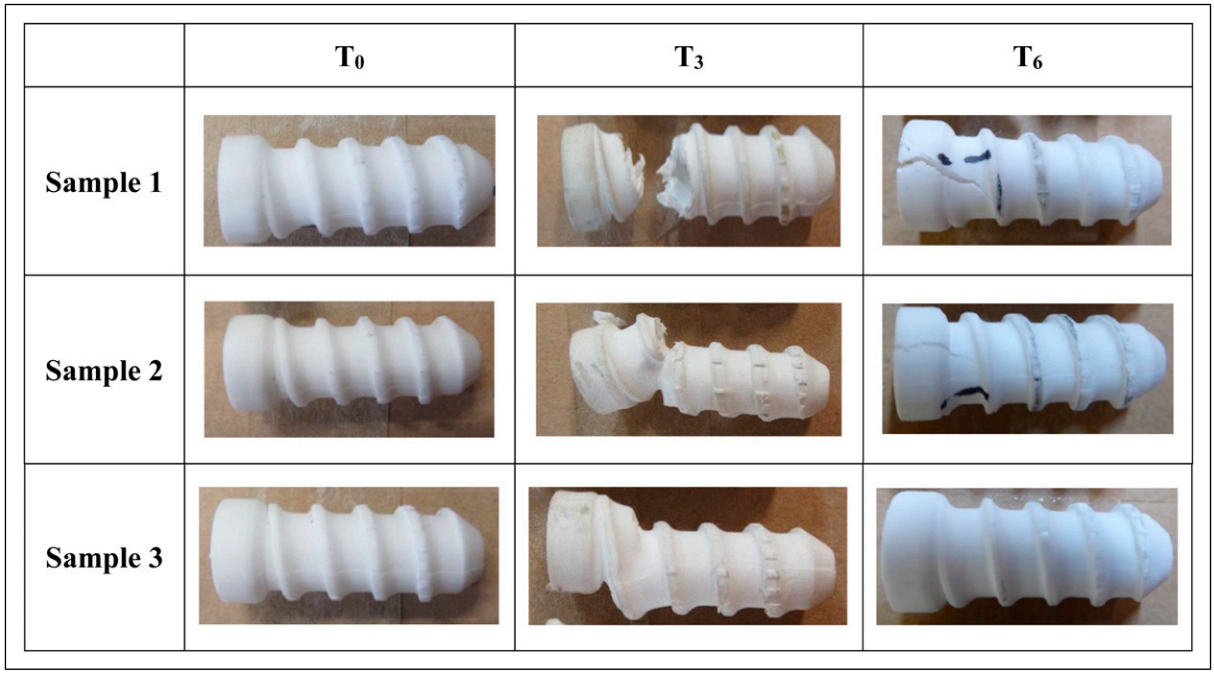

Figure 5. Images of three composite interference screws (Ø11–L30) used in static torsion test at T_0, T_3 and T_6.

tests and the image of this situation is shown in Figure 5. The reason for the non-breakage was stated as the screwdriver not being fixed in the screw and rotating. In other words, if a screwdriver is used that matches the profile and angles of the material being tested, the screwdriver will fit snugly against the screw surfaces, distributing the pressure evenly and the maximum torque results will be higher. In the Figure 5, the images of the screws after the torsion test at T_0, T_3 and T_6 are given. The fracture points are also clearly seen in the images.

Table 4 shows comparison chart with mechanical test results and acceptance criteria based on equivalent products on the market. It is seen that the composite screw prepared in the study has values between the accepted criteria.

Biological and safety testing

In vitro cytotoxic test of the interference screw test material against L-929 mammalian fibroblast cells by the direct contact method, the material does not exhibit cytotoxic properties. It is concluded that the test material is non-cytotoxic to L-929 mammalian fibroblast cells. Based on the results of the intracutaneous (intradermal) reactivity test, none of the animals treated with saline and sesame oil extracts of the test material showed a significantly greater reaction than animals treated with saline and sesame oil during the 72-h observation period. The saline and sesame oil extracts of the interference screw test material did not cause irritation to the skin of New Zealand White Rabbits as a result of the intracutaneous (intradermal) reactivity test.

Toxicity results in Swiss albino mice after intravenous and intraperitoneal administration of polar and non-polar extract of the test material indicated that all animals appeared normal and showed no clinical signs of intoxication during the 72 h observation period. None of the test animals showed any decrease in body weight. None of the animals treated with the extract of the test material showed a significantly higher biological reactivity than the animals treated with the untreated material.

Results of the pyrogenicity test study in which the interference screw test material was administered intravenously to rabbits, no individual animal showed a temperature increase of 0.5°C or more baseline temperature. No individual rabbit showed a temperature increase of 0.6°C and the total temperature increase of the three rabbits did not exceed 1.4°C.

In the study to determine the local effects of the interference screw 14 days after implantation into the rabbit femur bone, the test material did not cause death. All animals appeared normal and showed no clinical signs of intoxication after implantation until the end of the study. Post-mortem evaluation revealed no serious pathologic changes in any of the rabbits. The bone contact area and the amount of bone around the implant were evaluated macroscopically and microscopically for the presence of non-calcified tissues and inflammatory changes. In the macroscopic evaluation of toxicity, there was no encapsulation around the implanted test material and control material. Microscopic evaluation of toxicity showed inflammatory changes, fibrosis, fatty infiltration and traumatic necrosis. The interference screw test material showed no reaction at the implant sites in rabbit bone for 14 days after implantation.

Table 4. Comparison chart with mechanical test results and acceptance criteria based on equivalent products.

			Benchmark criteria		
Mechanical testing	Composite interference screw (Ø7–L30)	Composite interference screw (Ø11–L30)	Predicate device 1 (Ø7–L30)	Predicate device 2 (Ø7–L30)	Predicate device 3 (Ø6–L20)[50]
Maximum torque (N.m)	1.38 ± 0.05	6.6 ± 0.2	1.04 ± 0.07	0.98 ± 0.15	1.168 ± 0.016
Torsional yield strength (N.m)	1.31 ± 0.11	6.2 ± 0.6	0.86 ± 0.04	0.86 ± 0.01	1.073 ± 0.017

The guinea pig maximization test (GPMT) performed to determine the skin sensitization potential of the interference screw test material in albino guinea pigs, the interference screw did not cause skin sensitization in albino guinea pigs. The sensitization reaction score was 0.00. It was concluded that the interference screw test material is a substance that does not cause sensitization on the skin of albino guinea pigs.

The sub chronic systemic toxicity test performed all animals in the control and test groups were normal. No mortality and clinical signs were observed until the end of the 13 weeks study. There was no statistically significant difference between the control and test groups in terms of hematologic data (Hb, PCV, RBC, WBC, Platelet), blood chemistry parameters (SGPT, ALP, Glucose, Urea, Total Proteins), urine analysis, organ weights. No abnormal findings were observed when liver, kidney and bone tissues of the control and test groups were compared histologically. The interference screw test material showed no adverse effect in animals after implantation for 13 weeks in New Zealand White Rabbits. The genotoxicity test the interference screw test material did not cause cytotoxicity in CHO chinese hamster ovary cells. The cells showed no signs of toxicity in the vicinity of the sample. No clastogenicity was observed in the test material. The hemocompatibility test the haemolytic index of the material tested with human blood group A+, B+, 0+ is 1.68, 0.17, 2.07 respectively. The reverse mutation test performed, no mutagenicity was found in *Salmonella Typhimurium* TA 1535, TA 97a, TA 98, TA 100 and TA 102 strains of the interference screw.

Conclusion

In this study, composite interference screws were designed as fixation material in cruciate ligament injury. Design studies were carried out by following the literature under the guidance of ISO and ASTM standards. The interference screws were analysed physically, chemically, thermally, morphologically and biologically. It is concluded that they may provide better treatment conditions due to their mechanical strength and biodegradation. It has been observed that the they can provide better healing conditions due to parameters such as design, mechanical strength, biodegradability compared to equivalent products in the orthopaedics product market. The screw was introduced to the market and offered for implantation purposes to patients with specific disorders. It has taken a place as a product in the orthopaedics sector and presented the success of the studies.

Acknowledgments

We would like to thank BMT BAPS Biomaterial Co. for their infrastructural and financial support. We also would like to thank to TÜBİTAK (The Scientific and Technological Research Council of Turkey) for the financial support through the TÜBİTAK TEYDEB project (Project No: 7170647). Additionally, the authors would like to acknowledge the support provided by TÜBİTAK 1004 - Center of Excellence Support Prog - High Technology Platforms in Priority Fields (Project Number: 22AG004, *Next Generation Biomaterial Technologies Research Network for Healthy Life*).

ORCID iDs

Alkin Ozgen https://orcid.org/0009-0001-3593-7608
Orhan Gokalp Buyukuysal https://orcid.org/0000-0003-3597-3083
Halil Murat Aydin https://orcid.org/0000-0002-0732-1785

Funding

The authors disclosed receipt of the following financial support for the research, authorship, and/or publication of this article: This work was supported by the TÜBİTAK TEYDEB project (Project No: 7170647) and TÜBİTAK 1004 - Center of Excellence Support Prog - High Technology Platforms in Priority Fields (Project Number: 22AG004, *Next Generation Biomaterial Technologies Research Network for Healthy Life*).

Declaration of conflicting interests

The authors declared no potential conflicts of interest with respect to the research, authorship, and/or publication of this article.

Data Availability Statement

Data sharing not applicable to this article as no datasets were generated or analyzed during the current study.

Supplemental Material

Supplemental material for this article is available online.

References

1. Innocenti B. Chapter 13 - biomechanics of the knee joint. In: Innocenti B and Galbusera F (eds). *Human Orthopaedic Biomechanics*. Academic Press, 2022, pp. 239–263.
2. Zantop T, Petersen W and Fu FH. Anatomy of the anterior cruciate ligament. *Operat Tech Orthop* 2005; 15(1): 20–28.
3. Hartanti LPS, Bawono B, Yuniarto T, et al. Recent progress and perspective in material and manufacturing of interference screw. *Cogent Eng* 2024; 11(1): 2364048.
4. Zhang Z, Ortiz O, Goyal R, et al. 13 - biodegradable polymers. In: Modjarrad K and Ebnesajjad S (eds). *Handbook of Polymer Applications in Medicine and Medical Devices. Plastics Design Library*. William Andrew Publishing, 2014, pp. 303–335.
5. Fonseca AC, Serra AC and Coelho JFJ. Bioabsorbable polymers in cancer therapy: latest developments. *EPMA J* 2015; 6(1): 22.
6. Ramos DM, Dhandapani R, Subramanian A, et al. Clinical complications of biodegradable screws for ligament injuries. *Mater Sci Eng C* 2020; 109: 110423.
7. Konan S and Haddad FS. A clinical review of bioabsorbable interference screws and their adverse effects in anterior cruciate ligament reconstruction surgery. *Knee* 2009; 16(1): 6–13.
8. Sadiasa A, Sarkar SK, Franco RA, et al. Bioactive glass incorporation in calcium phosphate cement-based injectable bone substitute for improved in vitro biocompatibility and in vivo bone regeneration. *J Biomater Appl* 2013; 28(5): 739–756.
9. Eliaz N and Metoki N. Calcium phosphate bioceramics: a review of their history, structure, properties, coating technologies and biomedical applications. *Materials* 2017; 10(4): 334.
10. Dorozhkin SV and Epple M. Biological and medical significance of calcium phosphates. *Angew Chem Int Ed Engl* 2002; 41(17): 3130–3146.
11. Dorozhkin SV. Calcium orthophosphates as bioceramics: state of the art. *J Funct Biomater* 2010; 1(1): 22–107.
12. Okada M and Matsumoto T. Synthesis and modification of apatite nanoparticles for use in dental and medical applications. *Japanese Dental Science Review* 2015; 51(4): 85–95.
13. Armentano I, Dottori M, Fortunati E, et al. Biodegradable polymer matrix nanocomposites for tissue engineering: a review. *Polym Degrad Stabil* 2010; 95(11): 2126–2146.
14. Navarro M, Ginebra MP, Planell JA, et al. In vitro degradation behavior of a novel bioresorbable composite material based on PLA and a soluble CaP glass. *Acta Biomater* 2005; 1(4): 411–419.
15. Liu H, Slamovich EB and Webster TJ. Less harmful acidic degradation of poly (lactic-co-glycolic acid) bone tissue engineering scaffolds through titania nanoparticle addition. *Int J Nanomed* 2006; 1(4): 541–545.
16. Zhang R and Ma PX. Poly (alpha-hydroxyl acids)/hydroxyapatite porous composites for bone-tissue engineering. I. Preparation and morphology. *J Biomed Mater Res* 1999; 44(4): 446–455.
17. Kurosaka M, Yoshiya S and Andrish JT. A biomechanical comparison of different surgical techniques of graft fixation in anterior cruciate ligament reconstruction. *Am J Sports Med* 1987; 15(3): 225–229.
18. Caborn DNM, Urban WP, Johnson DL, et al. Biomechanical comparison between BioScrew and titanium alloy interference screws for bone—patellar tendon—bone graft fixation in anterior cruciate ligament reconstruction. *Arthroscopy* 1997; 13(2): 229–232.
19. Johnson LL and vanDyk GE. Metal and biodegradable interference screws: comparison of failure strength. *Arthroscopy* 1996; 12(4): 452–456.
20. Böstman O and Pihlajamäki H. Clinical biocompatibility of biodegradable orthopaedic implants for internal fixation: a review. *Biomaterials* 2000; 21(24): 2615–2621.
21. Nho SJ, Nam D, Ala OL, et al. Observations on retrieved glenoid components from total shoulder arthroplasty. *J Shoulder Elb Surg* 2009; 18(3): 371–378.
22. Böstman OM and Pihlajamäki HK. Adverse tissue reactions to bioabsorbable fixation devices. *Clin Orthop Relat Res* 2000; (371): 227. https://journals.lww.com/clinorthop/fulltext/2000/02000/adverse_tissue_reactions_to_bioabsorbable_fixation.26.aspx
23. Pietrzak WS and Kumar M. An enhanced strength retention Poly (Glycolic acid)-poly (l-lactic acid) copolymer for internal fixation: in vitro characterization of hydrolysis. *J Craniofac Surg* 2009; 20(5). https://journals.lww.com/jcraniofacialsurgery/fulltext/2009/09000/an_enhanced_strength_retention_poly_glycolic.48.aspx
24. Barber FA, Dockery WD and Hrnack SA. Long-term degradation of a poly-lactide Co-Glycolide/β-Tricalcium phosphate biocomposite interference screw. *Arthroscopy* 2011; 27(5): 637–643.
25. Ntagiopoulos PG, Demey G, Tavernier T, et al. Comparison of resorption and remodeling of bioabsorbable interference screws in anterior cruciate ligament reconstruction. *Int Orthop* 2015; 39(4): 697–706.
26. Barber FA, Dockery WD and Cowden CH. The degradation outcome of biocomposite suture anchors made from poly L-Lactide-Co-Glycolide and β-Tricalcium phosphate. *Arthroscopy* 2013; 29(11): 1834–1839.
27. Gritsch L, Perrin E, Chenal JM, et al. Combining bioresorbable polyesters and bioactive glasses: orthopedic applications of composite implants and bone tissue engineering scaffolds. *Appl Mater Today* 2021; 22: 100923.
28. Weiler A, Windhagen HJ, Raschke MJ, et al. Biodegradable interference screw fixation exhibits pull-out force and stiffness similar to titanium screws. *Am J Sports Med* 1998; 26(1): 119–126.
29. Kohn D and Rose C. Primary stability of interference screw fixation: influence of screw diameter and insertion torque. *Am J Sports Med* 1994; 22(3): 334–338.

30. Weiler A, Hoffmann RFG, Siepe CJ, et al. The influence of screw geometry on hamstring tendon interference fit fixation. *Am J Sports Med* 2000; 28(3): 356–359.
31. Brand JC, Pienkowski D, Steenlage E, et al. Interference screw fixation strength of a quadrupled hamstring tendon graft is directly related to bone mineral density and insertion torque. *Am J Sports Med* 2000; 28(5): 705–710.
32. Seil R, Rupp S, Krauss PW, et al. Comparison of initial fixation strength between biodegradable and metallic interference screws and a press-fit fixation technique in a porcine model. *Am J Sports Med* 1998; 26(6): 815–819.
33. Wozniak TD, Kocabey Y, Klein S, et al. Influence of thread design on bioabsorbable interference screw insertion torque during retrograde fixation of a soft-tissue graft in synthetic bone. *Arthroscopy* 2005; 21(7): 815–819.
34. dos Santos TMBK, Merlini C, Aragones Á, et al. Manufacturing and characterization of plates for fracture fixation of bone with biocomposites of poly (lactic acid-co-glycolic acid) (PLGA) with calcium phosphates bioceramics. *Mater Sci Eng C* 2019; 103: 109728.
35. Avgoustakis K. Polylactic-Co-Glycolic Acid (PLGA). In: Mishra, M. (Ed.), *Encyclopedia of biomaterials and biomedical engineering*, 2015; 11. 1st ed. CRC Press. DOI: 10.1081/E-EBBE-120013950.
36. Middleton JC and Tipton AJ. Synthetic biodegradable polymers as orthopedic devices. *Biomaterials* 2000; 21(23): 2335–2346.
37. Sin LT. *Polylactic acid: PLA biopolymer technology and applications*. William Andrew, 2012.
38. Van de Velde K and Kiekens P. Biopolymers: overview of several properties and consequences on their applications. *Polym Test* 2002; 21(4): 433–442.
39. Castro VO, Fredel MC, Aragones Á, et al. Electrospun fibrous membranes of poly (lactic-co-glycolic acid) with β-tricalcium phosphate for guided bone regeneration application. *Polym Test* 2020; 86: 106489.
40. Kim J, McBride S, Tellis B, et al. Rapid-prototyped PLGA/β-TCP/hydroxyapatite nanocomposite scaffolds in a rabbit femoral defect model. *Biofabrication* 2012; 4(2): 025003.
41. Wong-Ng W, McMurdie HF, Hubbard CR, et al. JCPDS-ICDD research associateship (cooperative program with NBS/NIST). *J Res Natl Inst Stand Technol* 2001; 106(6): 1013–1028.
42. Luo YR, Zhang L, Chen C, et al. The delayed degradation mechanism and mechanical properties of β-TCP filler in poly (lactide-co-glycolide)/beta-tricalcium phosphate composite suture anchors during short-time degradation in vivo. *J Mater Res* 2018; 33(24): 4278–4286.
43. Vorokh AS. Scherrer formula: estimation of error in determining small nanoparticle size. *Nanosystems: Phys Chem Math*. 2018; 9(3): 364–369. doi:10.17586/2220-8054-2018-9-3-364-369
44. Dong W, Huang X, Sun Y, et al. Mechanical characteristics and in vitro degradation kinetics analysis of polylactic glycolic acid/β-tricalcium phosphate (PLGA/β-TCP) biocomposite interference screw. *Polym Degrad Stabil* 2021; 186: 109421.
45. Gentile P, Chiono V, Carmagnola I, et al. An overview of poly (lactic-co-glycolic) acid (PLGA)-based biomaterials for bone tissue engineering. *Int J Mol Sci* 2014; 15(3): 3640–3659.
46. Loher S, Reboul V, Brunner TJ, et al. Improved degradation and bioactivity of amorphous aerosol derived tricalcium phosphate nanoparticles in poly (lactide-co-glycolide). *Nanotechnology* 2006; 17(8): 2054–2061.
47. Darestani FT, Abtahi M, Entezami AA, et al. Degradition of poly (D, L-Lactide-CO-Glycolide) 50: 50. *Iran Polym J (Engl Ed)* 2005.
48. Niemelä T. Effect of β-tricalcium phosphate addition on the in vitro degradation of self-reinforced poly-l,d-lactide. *Polym Degrad Stabil* 2005; 89(3): 492–500.
49. Lin L, Wang T, Zhou Q, et al. The effects of different amounts of drug microspheres on the vivo and vitro performance of the PLGA/β-TCP scaffold. *Des Monomers Polym* 2017; 20(1): 351–362.
50. Roesler CRM, Salmoria GV, Moré ADO, et al. Torsion test method for mechanical characterization of PLDLA 70/30 ACL interference screws. *Polym Test* 2014; 34: 34–41.